Fax to: +4930/82787-5643

Christel Pierru
Springer-Verlag GmbH & Co. KG, Berlin

From:

Re: **Electrical Engineering DOI 10.1007/s00202-003-0178-2**
Some important aspects of oil power transformer thermal protection

Authors: **Radakovic · Feser**

I. Permission to publish

Dear Christel Pierru,

I have checked the proofs of my article and

- ❑ I have **no corrections.** The article is ready to be published without changes.
- ❑ I have **a few corrections.** I am enclosing the following pages:
- ❑ I have made **many corrections.** Enclosed is the **complete article.**

II. Offprint order

❑ Offprint order enclosed ❑ I do not wish to order offprints

Remarks:

Date / signature ____________________

III. Copyright Transfer Statement (sign only if not submitted previously)

Date / Author's signature ____________________

Journal: Electrical Engineering
DOI: 10.1007/s00202-003-0178-2

Offprint Order Form

- To determine if your journal provides free offprints, please check the journal's instructions to authors.
- You are entitled to a PDF file **if you order offprints.**
- Please checkmark where to send the PDF file:

❑ radako@ieh.uni-stuttgart.de

❑ ____________________

- If you do not return this order form, we assume that you do not wish to order offprints.
- If you order offprints **after** the issue has gone to press, costs are much higher. Therefore, we can supply offprints only in quantities of 300 or more after this time.
- For orders involving more than 500 copies, please ask the production editor for a quotation.

Please enter my order for:

	Copies	Price EUR	Price USD
❑	50	300.00	292.50
❑	100	350.00	340.00
❑	200	475.00	465.00
❑	300	600.00	585.00
❑	400	725.00	705.00
❑	500	850.00	825.00

Prices include surface mail postage and handling. Customers in EU countries who are not registered for VAT should add VAT at the rate applicable in their country.

VAT registration number (EU countries only):

____

I wish to be charged in
❑ Euro
❑ US-Dollar

If not specified, invoices are made out in Euro.

Please indicate your institutional purchase order number (if any) here

____

and send the purchase order, with all information about the article, via regular mail. The author will be billed for orders without a purchase order number. The title of the journal and the manuscript number of the article must be stated on the purchase order.

❑ Please charge my credit card
  ❑ Eurocard/Access/Mastercard
  ❑ American Express
  ❑ Visa/Barclaycard/BankAmericard

Number (incl. check digits):

_ _ _ _ _ _ _ _ _ _ _ _ _ _ _ _ _ _ _

Valid until: _ _ / _ _

Signature: ____________________

Send invoice to:

❑ Z. Radakovic
Univ. Stuttgart
Inst. Energieübertragung und
Hochspannungstechnik
47 Pfaffenwaldring
Stuttgart
70569, Germany

❑ ____________________

Ship offprints to:

❑ Z. Radakovic
Univ. Stuttgart
Inst. Energieübertragung und
Hochspannungstechnik
47 Pfaffenwaldring
Stuttgart
70569, Germany

❑ ____________________

Date / signature: ____________________

Electrical Engineering

DOI 10.1007/s00202-003-0178-2

Some important aspects of oil power transformer thermal protection

Z. Radakovic (✉) · K. Feser

Z. Radakovic · K. Feser
Institute for Power Transmission and High-voltage Technology, University of Stuttgart, Pfaffenwaldring 47, 70569 Stuttgart, Germany

✉ Z. Radakovic
Phone: +49-(0
E-mail: radako@ieh.uni-stuttgart.de

Received: 24 March 2003 / **Accepted:** 15 May 2003

Abstract The original transient thermal model of transformers with ONAN cooling was developed in a previous work by the authors. The parameters of the model are determined from inexpensive measurements in the short-circuit heating experiment. Two problems exist in the on-line application of the model: unknown starting hot-spot temperature and variation in the thermal parameters in a long-term transformer operation. Both are discussed in this paper, and the solution through the application of a thermal observer is also discussed.

Key words Thermal protection · Oil power transformer · Hot-spot · Loading · Thermal model · Observer

1 Introduction

The hot-spot insulation temperature represents the most important limiting factor of a transformer loading. There is interest in knowing the hot-spot temperature at every moment of a real transformer operation in conditions of variable load and ambient air temperature. Possible approaches are to measure the hot-spot temperature (using a fibre-optics technique) or to calculate it, using a thermal model of a power transformer.

The originally developed algorithm (thermal model) for temperature calculation [1] delivers one characteristic local temperature in windings and one characteristic temperature in oil. The algorithm is established on the following two fundamentals:

1. To describe as much as possible the real physics of heat transfer, an improvement is made in processing the influence of non-linear heat transfer characteristics to the transient thermal behaviour.
2. To determine the thermal model parameters for a specific transformer type without complicated and expensive measurements (in contrast to the models from [2, 3]).

The thermal characteristics of a transformer can change in long-term transformer operation. Therefore, the thermal parameters of the model may be different from the values initially determined experimentally in the short-circuit heating experiment. Incorrect parameter values in the model can lead to an error in temperature calculation. The only practically acceptable method for detecting parameters variation is to monitor the oil temperature.

Another problem in the model application is the unknown initial value of the hot-spot temperature. To speed up the elimination of the error caused by the estimated initial hot-spot temperature, a thermal observer can be used. Introduction of a thermal observer leads to implications in the calculation of the hot-spot and the oil temperatures. Consequently, it affects the detection of changes in the thermal model parameters. This paper analyses all aspects of the thermal observer. The experimental basis of the research are the measurements on a 630 kVA, 3×10 kV/3×6 kV ONAN transformer equipped with a large number of sensors for local temperature measurements [4].

2 Short description of the original thermal model

The thermal model is based on the thermal network shown in Fig. 1. Characteristic temperature rises are calculated with respect to the temperature of the air surrounding the transformer.

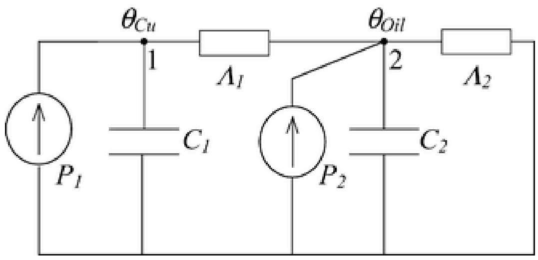

Fig. 1. The thermal network with two nodes

The system is non-linear due to the temperature-dependent thermal conductances. The most convenient and commonly used [5] dependences are:

$$\Lambda_1 = K_1(\theta_{\mathrm{Cu}} - \theta_{\mathrm{Oil}})^{n_1} \tag{1}$$

$$\Lambda_2 = K_2(\theta_{\mathrm{Oil}})^{n_2} \tag{2}$$

The parameters K_1, n_1, K_2, n_2, C_1 and C_2 are determined by the procedure developed [1] from the values of measured characteristic temperatures in the short-circuit heating experiment. As explained in detail in [4], the most convenient characteristic temperatures are those of the hot-spot and the bottom oil. The definition of the hot-spot temperature during the short-circuit experiment, based on easily measured temperatures, is also developed and described in [4].

The power loss distribution in the short-circuit heating experiment and during normal transformer operation is considered in [6].

Temperature rises θ_{Cu} and θ_{Oil} in discrete time (multiple of period T) can be calculated from the difference equations representing the energy balance for nodes 1 and 2 [4]. The initial values of θ_{Cu} and θ_{Oil} should be specified in order to carry out the procedure. The initial copper temperature θ_{Cu} is not known and can be set arbitrarily. The error in θ_{Cu} calculation caused by the incorrect initial value disappears in time as a consequence of the system characteristics. To speed up and control a reduction in this error, an observer structure can be used.

3 Theoretical consideration of the thermal observer

The observer enables the calculation of non-measurable system states, using measurable system outputs. The observer is a numerical structure containing the mathematical model of the system. The non-measurable states of the real system are accessible from the model contained in the observer. The initial values of the non-measurable states in the model should be set as close as possible to the corresponding values in the real system. The difference in states of the model and of the real system should be eliminated as soon as possible. The real system, the model of the system “inside” the observer and their “coupling” feedback represent one dynamic structure. The dynamics of error elimination are determined by all the parameters of the structure, i.e. they can be controlled by adjusting the feedback parameters. The configuration of the applied thermal observer is shown in Fig. 2.

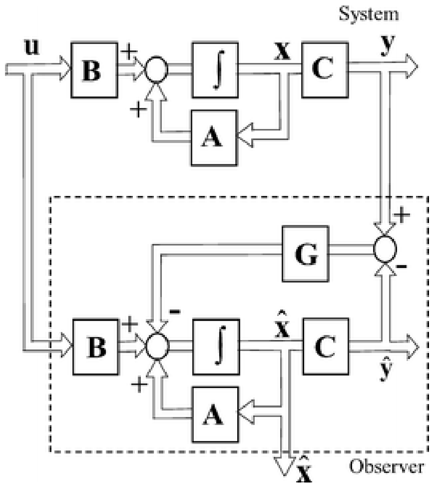

Fig. 2. Block diagram of the thermal system with observer

The basic observer theory is established under the assumption that the mathematical model of the system is known and precise. In the case where the model disagrees with the real system, the results of the observer application are strongly influenced by the precision of modelling. This has to be considered carefully.

It should be noted that the non-measurable states could be obtained using a model of the real system only, i.e. without coupling feedback. In this case, the dynamics of error elimination cannot be controlled and are determined by the self-response of the system.

3.1 Mathematical model of the system with observer

Using the node potential method, applied to the network in Fig. 1, the continuous state equation of a transformer can be written as

$$\dot{\mathbf{x}} = \mathbf{A}_\mathrm{c}(x_1, x_2)\mathbf{x} + \mathbf{B}_\mathrm{c}\mathbf{u} \tag{3}$$

$$\mathbf{y} = \mathbf{C}_\mathrm{c}\mathbf{x} + \mathbf{D}_\mathrm{c}\mathbf{u} \tag{4}$$

where

$$\begin{gathered}\mathbf{x} = \begin{bmatrix}\theta_\mathrm{Cu}\\ \theta_\mathrm{Oil}\end{bmatrix};\ \mathbf{u} = \begin{bmatrix}P_\mathrm{Cu}\\ P_\mathrm{Fe}\end{bmatrix};\ \mathbf{y} = \theta_\mathrm{Oil};\\ \mathbf{A}_\mathrm{c} = \begin{bmatrix}-\frac{\Lambda_1(\theta_\mathrm{Cu},\theta_\mathrm{Oil})}{C_1} & \frac{\Lambda_1(\theta_\mathrm{Cu},\theta_\mathrm{Oil})}{C_1}\\ \frac{\Lambda_1(\theta_\mathrm{Cu},\theta_\mathrm{Oil})}{C_2} & -\frac{\Lambda_1(\theta_\mathrm{Cu},\theta_\mathrm{Oil})+\Lambda_2(\theta_\mathrm{Oil})}{C_1}\end{bmatrix}; \mathbf{B}_\mathrm{c} = \begin{bmatrix}\frac{1}{C_1} & 0\\ 0 & \frac{1}{C_2}\end{bmatrix};\\ \mathbf{C}_\mathrm{c} = [0 \quad 1]; \mathbf{D}_\mathrm{c} = [0 \quad 0]\end{gathered} \tag{5}$$

The most suitable way of defining elements of matrices **A** and **B** in the discrete state equation with the form

$$\mathbf{x}[(k+1)T] = \mathbf{A}(\mathbf{x})\mathbf{x}(kT) + \mathbf{B}(\mathbf{x})\mathbf{u}(kT) \tag{6}$$

$$\mathbf{y}(kT) = Cx(kT) + \mathbf{D}\mathbf{u}(kT) \tag{7}$$

is by computer evaluation:

$$\mathbf{A}(\mathbf{x}) = \mathbf{I} + \mathbf{A}_{\mathrm{c}}(\mathbf{x})T + \mathbf{A}_{\mathrm{c}}(\mathbf{x})^2\frac{T^2}{2!} + \mathbf{A}_{\mathrm{c}}(\mathbf{x})^3\frac{T^3}{3!} + ... \tag{8}$$

$$\mathbf{B}(\mathbf{x}) = T\left(\mathbf{I} + \mathbf{A}_{\mathrm{c}}(\mathbf{x})\frac{T}{2!} + \mathbf{A}_{\mathrm{c}}(\mathbf{x})^2\frac{T^2}{3!} + \mathbf{A}_{\mathrm{c}}(\mathbf{x})^3\frac{T^3}{4!} + ...\right)\mathbf{B}_{\mathrm{c}} \tag{9}$$

where T is the sampling period. Equations (8) and (9) are written under the real assumption that the sampling period T is significantly shorter than the thermal time constants. Consequently, the matrix $\mathbf{A}_{\mathrm{c}}(\mathbf{x})$ can be considered constant during the sampling period T. Matrices **C** and **D** are equal to $\mathbf{C}_{\mathrm{c}}$ and $\mathbf{D}_{\mathrm{c}}$, respectively.

The discrete state equations of the observer, shown in Fig. 2, are

$$\hat{\mathbf{x}}[(k+1)T] = \mathbf{A}(\hat{\mathbf{x}})\hat{\mathbf{x}}(kT) + \mathbf{B}(\hat{\mathbf{x}})\mathbf{u}(kT) + \mathbf{G}[\mathbf{y}(kT) - \hat{\mathbf{y}}(kT)] \tag{10}$$

$$\hat{\mathbf{y}}(kT) = \mathbf{C}\hat{\mathbf{x}}(kT) \tag{11}$$

The error vector $\mathbf{e}(kT)$ is defined as

$$\mathbf{e}(kT) = \mathbf{x}(kT) - \hat{\mathbf{x}}(kT) \tag{12}$$

From the observer state equation, derived from (10) and (11)

$$\hat{\mathbf{x}}[(k+1)T] = [\mathbf{A}(\hat{\mathbf{x}}) - \mathbf{G}\mathbf{C}]\hat{\mathbf{x}}(kT) + \mathbf{B}(\hat{\mathbf{x}})\mathbf{u}(kT) + \mathbf{G}\mathbf{y}(kT) \tag{13}$$

and (6) and (7), the error vector $\mathbf{e}[(k+1)T]$ is equal to

$$\begin{aligned} \mathbf{e}[(k+1)T] &= \mathbf{x}[(k+1)T] - \hat{\mathbf{x}}[(k+1)T] \\ &= \mathbf{A}(\mathbf{x})\mathbf{x}(kT) + \mathbf{B}(\mathbf{x})\mathbf{u}(kT) - [\mathbf{A}(\hat{\mathbf{x}}) - \mathbf{G}\mathbf{C}]\hat{\mathbf{x}}(k) - \mathbf{B}(\hat{\mathbf{x}})\mathbf{u}(kT) - \mathbf{G}\mathbf{C}\mathbf{x}(kT) \end{aligned} \tag{14}$$

Under the assumptions $\mathbf{A}(\hat{\mathbf{x}}) = \mathbf{A}(\mathbf{x})$ and $\mathbf{B}(\hat{\mathbf{x}}) = \mathbf{B}(\mathbf{x})$, Eq. (14) becomes

$$\mathbf{e}[(k+1)T] = [\mathbf{A}(\mathbf{x}) - \mathbf{GC}][\mathbf{x}(kT) - \hat{\mathbf{x}}(kT)] = [\mathbf{A}(\mathbf{x}) - GC]\mathbf{e}(kT) \tag{15}$$

If, instead of the matrix **A** dependent on states **x**, the matrix **A** were constant, the error dynamics could be described by the following characteristic equation

$$|z\mathbf{I} - (\mathbf{A} - \mathbf{GC})| = 0 \tag{16}$$

where z is the discrete complex operator. By adjusting the gains of the column-vector **G**, the error dynamics can be tuned [7]. Since the observer is of the second order, gains g_1 and g_2 can be obtained by solving two equations with two unknowns. If the elements of matrix **A** are denoted by

$$\mathbf{A} = \begin{bmatrix} a_{11} & a_{12} \\ a_{21} & a_{22} \end{bmatrix}$$

and the designed poles of error dynamics are, for example, equal, real and positive, denoted by z_p, the gains are

$$g_2 = a_{11} + a_{22} - 2z_\mathrm{p} \tag{17}$$

$$g_1 = \frac{1}{a_{21}}(z_\mathrm{p}^2 - a_{11}a_{22} + a_{12}a_{21} + a_{11}g_2) \tag{18}$$

3.2 Real case discrepancies

The mathematical model presented in the above subsection describes an idealised case. The first discrepancy is that the thermal behaviour of the transformer cannot be perfectly described by Eqs. (3), (4) and (5), i.e. the model in the observer does not fully match the system. The second discrepancy is that matrix **A** is the function of states, disabling the correct application of the linear system theory. The third problem to be considered is the presence of oil temperature and current measurement noise, i.e. power loss noise, in the practical application. Also, the change in thermal parameters during the long-term operation of the transformer should be analysed.

The general recommendation [7] is that the gains of vector **G** should be larger if the unknowns are significant and smaller if measuring noise is significant; it is recommended that an accurate simulation is used to find the optimal values of gains regarding unknowns and measuring noise.

4 Tests of the observer by constant thermal parameters

This first group of tests investigated the influence of non-linearity, non-ideal transformer thermal modelling and measuring noise. The first step was to test the incorrectness of the linear theory application to the non-linear case. The second step was to test the application of the observer on a real transformer. In that way, a separation of specific real-case disturbance factors was made.

4.1 Parameters of the tested transformer

As shown in [4], the thermal conductances of the 630 kVA transformer tested, with hot-spot and bottom oil characteristic temperatures, are

- $\Lambda_1=16.224(\vartheta_{hs}-\vartheta_{bo})^{0.60454}$ and
- $\Lambda_2=294.302(\theta_{bo})^0=294.30$.

It is interesting to note that, although the transformer has ONAN cooling, thermal conductance Λ_2 appears to be constant. The thermal capacitances are $C_1=185.6$ kJ/K and $C_2=2631$ kJ/K [4]. Rated power losses in copper amount to $P_{Cu\,r}=8{,}790$ W and in iron $P_{Fe\,r}=1{,}875$ W. It means that the rated temperature rises are: the bottom oil $\theta_{bo\,r}=36.2$ K and the hot-spot $\theta_{hs\,r}=86.8$ K. The corresponding rated values of thermal conductances are $\Lambda_{1\,r}=173.85$ W/K and $\Lambda_{2\,r}=294.30$ W/K. The sampling period for measurement and calculation is $T=20$ s, yielding 180 values of both temperatures in an hour.

4.2 The influence of non-linearity

The tests were performed as follows. The elements of vector **G** were calculated by Eqs. (17) and (18), i.e. the observer is designed assuming that the system is linear. The constant matrix **A** is calculated by (8), where $\mathbf{A}_c$ is assumed to be constant. The values of matrix $\mathbf{A}_c$ are calculated by (5), using constant thermal conductances $\Lambda_1(\theta_{Cu}, \theta_{Oil})=\Lambda_{1\,r}$ and $\Lambda_2(\theta_{Cu}, \theta_{Oil})=\Lambda_{2\,r}$:

$$A_c = A_c^* = \begin{bmatrix} -\frac{173.8}{185.6} & \frac{173.8}{185.6} \\ \frac{173.8}{2631} & -\frac{173.8+294.3}{185.6} \end{bmatrix} 10^{-3}$$

Two different groups of calculations were made: the first with the behaviour of transformer ("System" in Fig. 2) simulated by non-linear equations

$$A_c = A_c^{**} = \begin{bmatrix} -\frac{16.224(\vartheta_{hs}-\vartheta_{bo})^{0.60454}}{185.6} & \frac{16.224(\vartheta_{hs}-\vartheta_{bo})^{0.60454}}{185.6} \\ \frac{16.224(\vartheta_{hs}-\vartheta_{bo})^{0.60454}}{2631} & -\frac{(16.224(\vartheta_{hs}-\vartheta_{bo})^{0.60454}+294.3)}{185.6} \end{bmatrix} 10^{-3}$$

and the second simulated by linear equations, $\mathbf{A_c}=\mathbf{A_c^*}$. In both groups of calculations, matrices **A** and **B** in the observer structure are the same as in the equations used to simulate the transformer. The test load diagram is shown in Fig. 3.

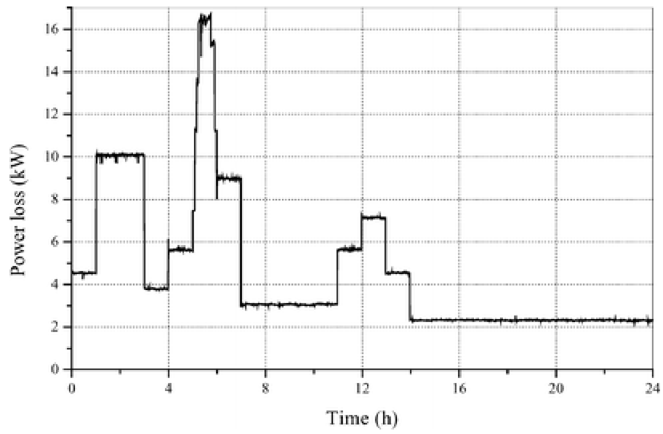

Fig. 3. The test load losses diagram

The results of calculations are given in Table 1. The initial difference between the supposed and real hot-spot temperatures was 21.2 K.

[Table 1. will appear here. See end of document.]

Figure 4 shows the simulated hot-spot temperatures delivered by the non-linear equations of a transformer and by the observer, as well as the time decreasing difference. It should be noted that the error drops below 0.2 K after 0.92 h, and is practically zero during the rest of the simulation. That is why only the first two hours of the test are shown in Fig. 4. The good tracking is the consequence of the same mathematical model used inside the "System" and "Observer" structures.

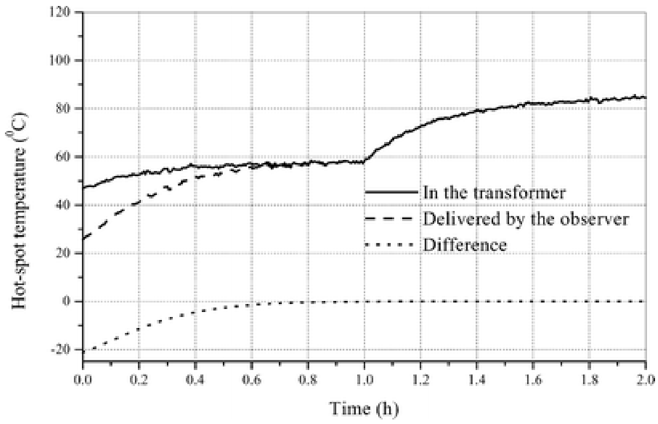

Fig. 4. Operation of the observer (τ=10 min) with the transformer simulated by non-linear equations

The results given in Table 1 show that the influence of non-linearity is not negligible, but small: the decrease in hot-spot temperature error is somewhat faster, and the action of the observer, expressed through the values of $RMSE_{1\ h}$, is somewhat stronger in the linear model.

4.3 The influence of non-ideal transformer modelling and measuring noise

In this group of tests, the real measurements on the transformer were used. In the "Observer" structure, matrices **A** and **B** were calculated based on variable conductances, i.e. the functional dependence of matrices **A** and **B** of states is included. The values of gain vector **G** were calculated as in Sect 4.2. The results of the calculations for the test load diagram in Fig. 3 and initial hot-spot temperature error of 21.2 K are given in Table 2.

[Table 2. will appear here. See end of document.]

The observer dynamics in eliminating the initial hot-spot temperature error did not change conspicuously compared with cases from Sect. 4.2. The values of *RMSE* and maximum bottom-oil temperature differences have grown extensively. The use of the observer increased the hot-spot calculation error compared with the situation when only the thermal model was used; the stronger feedback of the observer gives a greater hot-spot temperature error. It means that the observer produced the opposite effect to the desired one. Further investigations confirmed such a conclusion—the series of experiments (one-step load increase or decrease, short-time overload, intermittent duty) is described in [1].

5 The tests with variable thermal parameters

5.1 Using the observer

Two tests with the adopted time constant τ=10 min and the test diagram in Fig. 3 were performed. The first was with the transformer simulated by the non-linear equations ($\mathbf{A}_c = \mathbf{A}_c^{**}$). The influence of the worsening of the transformer cooling system is modelled by the decrease in the thermal conductances Λ_1 and Λ_2. Matrices **A** and **B** in the observer structure are calculated with the non-decreased thermal conductances Λ_1 and Λ_2 (x=1); the results are shown in Table 3.

[Table 3. will appear here. See end of document.]

The second test was perfomed using the real measurements on the transformer [4]. Since the thermal characteristics of the transformer were constant during the measurements, the tests of their worsening were made by increasing the thermal conductancies in matrices **A** and **B** in the "Observer" structure. The results are shown in Table 4.

[Table 4. will appear here. See end of document.]

As expected, the change in copper to oil thermal conductance Λ_1 does not lead to a significant change in *RMSE* values and cannot be detected by monitoring the *RMSE* function. The change in this conductance leads to a strong change in the maximum calculation error of the hot-spot temperature. With the transformer simulated by the non-linear equations, the hot-spot temperature error rises with the decrease in Λ_1. With the real transformer, the hot-spot temperature error course is not clear.

The change in oil to air thermal conductance Λ_2 leads to a noticeable change in *RMSE* values and could be detected by monitoring the *RMSE* function. The maximum calculation error of hot-spot temperature also increases.

5.2 Identification without using the observer

The hot-spot and bottom oil temperatures are calculated using the thermal model of transformer only, i.e. Eqs. (6) and (7), and are compared with the measured temperatures. The influence of the worsening of the transformer thermal characteristics is modelled by increasing the thermal conductances in the thermal model. The results are shown in Table 5.

[Table 5. will appear here. See end of document.]

Due to the absence of oil temperature feedback, the oil temperature difference and *RMSE* values are much higher than in the case where the observer is used. Regarding the possibility of detection of a change in thermal parameters , similar conclusions remain as in the case of observer application.

5.3 Final consideration

An overview of the change in the $RMSE_{24\,\mathrm{h}}$ caused by the change in thermal characteristics is shown in Figs. 5 and 6. For all three cases examined, described in detail in Sects. 5.1 and 5.2, the values of $RMSE_{24\,\mathrm{h}}$ are expressed relative to the $RMSE_{24\,\mathrm{h}}$ value for the non-decreased thermal conductances (x=1). In such a way, the sensitivity of the $RMSE_{24\,\mathrm{h}}$ function to the change in thermal parameters can be quantified.

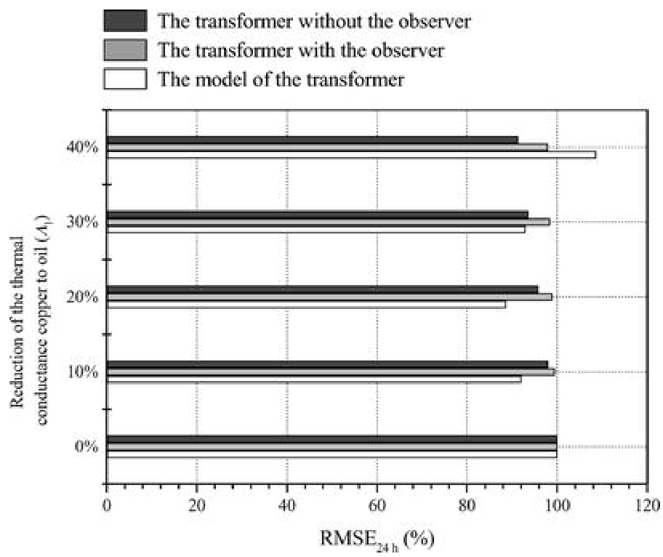

Fig. 5. The $RMSE_{24\,h}$ as a function of the change in Λ_1

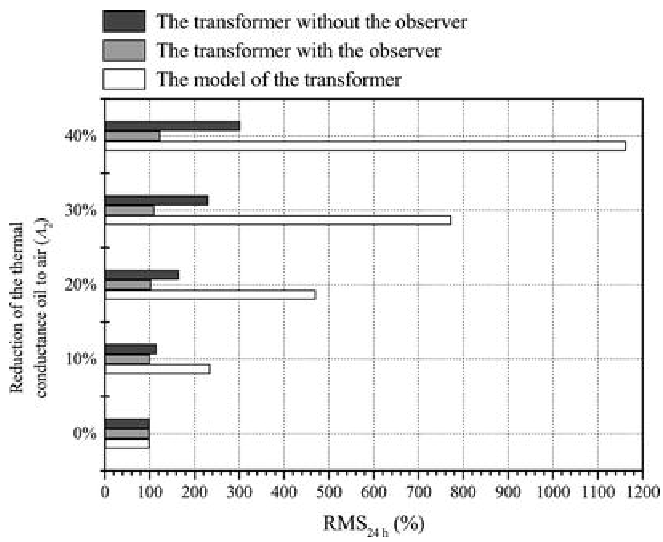

Fig. 6. The $RMSE_{24\,h}$ as a function of the change in Λ_2

In all three cases, the value of $RMSE_{24\,h}$ is not influenced by the change in windings to oil heat conductance Λ_1. This can be explained using the physics of the heat process. The "time constant" of the thermal process in copper is much shorter than the "time constant" of the process in oil. Hence, the change in Λ_1, i.e. the dynamics of transfer of power losses generated in copper does not conspicuously affect the oil temperature and the value of $RMSE_{24\,h}$. In practice, worsening of the windings to oil heat transfer can happen due to the closing of the cooling channels inside the windings or due to reduced oil flow caused by increased hydraulic resistance (as a consequence of the sedimentation of substance from the oil, especially on parts with small cross-sections).

Since the value of $RMSE_{24\,h}$ changes strongly with the change in oil to air heat conductance Λ_2, the change in corresponding heat transfer can be detected. The relative values of $RMSE_{24\,h}$ are very large in the case of a transformer simulated by non-linear equations, since the base value (with $x=1$) is very small. The oil temperature feedback using the observer on the real transformer causes not only absolute lower values of $RMSE_{24\,h}$, but also lower relative values, compared with the case when no observer is used. The change in Λ_2 can occur in practice due to the outage of certain parts of radiators or the sedimentation of a substance to the inner and outer radiator surfaces. The second factor is very important in transformers with high power density per heat exchanger surface; detailed practical analysis for the transformer with OFWF cooling is given in [8].

In addition to the possibility of detecting the change in oil to air heat transfer, the correction of the corresponding thermal conductance in the model, i.e. adapting the thermal model, can be done. The method presented in [9] can be applied. Because the oil temperature is measured, actual oil to air thermal conductance is of principal importance for the evaluation of the possibility of transformer overload.

Since the change in Λ_1 cannot be detected, it is important to analyse the influence on error in the calculated hot-spot temperature. The precision of the hot-spot temperature calculation is higher without the observer, compared with the calculation with the observer in the range of the change in Λ_1 below 16%, as shown in Fig. 7.

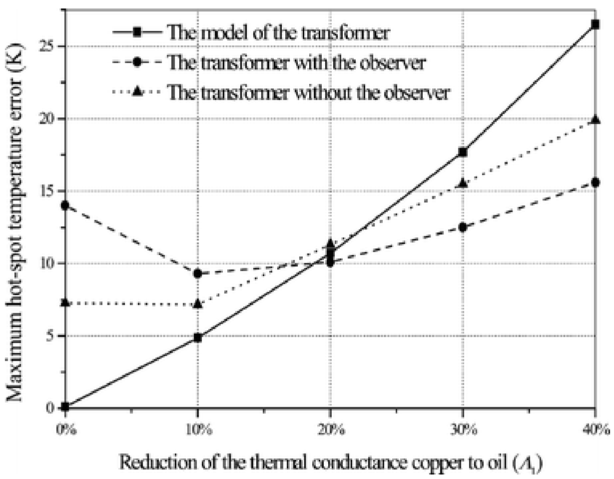

Fig. 7. The calculation error of the hot-spot temperature as a function of the change in Λ_1

6 Conclusions

The use of the proposed applied observer leads to expected faster elimination of difference between initial estimated and real hot-spot temperatures. Unfortunately, it also leads to reduced precision of hot-spot temperature calculation during normal transformer operation. The importance of precision is obvious, since the protection of the transformer is based on the calculated value of hot-spot temperature. The reduced precision is caused by an insufficiently accurate transformer thermal model and existing measuring noise.

In practice, the use of a thermal observer could be avoided, i.e. the thermal model alone could be used. As a consequence, the calculation error of the hot-spot temperature at the beginning of the calculation process (for example, during the first hour) would be too high. Fortunately, the start of the calculation process is of practical interest only after resetting the microprocessor relay, along with the temperature inside the transformer being higher than the ambient temperature.

The measured state variable, oil temperature, is not strongly influenced by a change in thermal conductance describing copper to oil heat transfer. Therefore, it is difficult to detect the change in this heat transfer. The same holds for both applied identification techniques: with and without observer. In contrast, the change in oil to air heat transfer is easy to detect.

The thermal observer applied cannot be used as the complete solution for all the practical problems in transformer thermal protection and evaluation of the possibility of overload. The observer can be used to speed up the elimination of the initial calculation error (delivering results applicable for protection in a shorter period). After the initial period, the thermal model alone gives higher hot-spot temperature precision and should substitute the observer. Future work could make an attempt with other observer structures, exposed to the tests described in this paper. On the best observer structure, further experiments on a transformer with variable thermal characteristics could be conducted.

Acknowledgement The research was supported by the Alexander von Humboldt Foundation.

References

1. Radakovic Z, Kalic Dj (1997) Results of a novel algorithm for the calculation of the characteristic temperatures in power oil transformers. Electr Eng 80:205–214
2. Pierce LW (1992) An investigation of the thermal performance of an oil filled transformer winding. IEEE Trans Power Delivery 7:1347–1358

3. Aubin J, Langhame Y (1992) Effect of oil viscosity on transformer loading capability at low ambient temperatures. IEEE Trans Power Delivery 7:516–524
4. Radakovic Z, Feser K (in press) A new method for the calculation of the hot-spot temperature in power transformers with ONAN cooling. To appear in IEEE Trans Power Delivery
5. IEC (1991) Loading guide for oil immersed transformers, IEC Standard, Publication 354, 2nd edn
6. Radakovic Z (2003) Numerical determination of characteristic temperatures in directly loaded power oil transformer. Eur Trans Electr Power 13:47–54
7. Phillips CL, Nagle HT (1984) Digital control system analysis and design, 3rd edn. Prentice-Hall, London
8. Radakovic Z, Popovic A (2003) Variation of steady-state thermal characteristics of transformers with OFWF cooling in service. Electr Power Compon Syst 31(8)
9. Radakovic Z, Maksimovic S (2002) Non-stationary thermal model of indoor transformer stations. Electr Eng 84:109–117

Table 1. The influence of non-linearity

	τ (min)	t_{er} (min)	$RMSE_{1\,h}$ (K)	$\Delta\theta_{bo\,max}$ (K)
Non-linear	1	3.33	0.0064	<0.1
Linear		2.33	0.0075	<0.1
Non-linear	2	5.67	0.0159	<0.1
Linear		4.33	0.0179	<0.1
Non-linear	3	8.0	0.0284	<0.1
Linear		6.33	0.0312	0.10
Non-linear	4	9.66	0.0433	0.11
Linear		8.0	0.0467	0.13
Non-linear	5	11.66	0.0603	0.14
Linear		9.33	0.0641	0.16
Non-linear	10	17.66	0.1718	0.29
Linear		15.33	0.1754	0.32
Non-linear	15	20.0	0.3150	0.46
Linear		17.66	0.3165	0.47
Non-linear	20	20.0	0.4717	0.62
Linear		18.0	0.4728	0.62
Non-linear	**G=0** (no observer)	21.0	0.9077	1.09
Linear		19.0	0.9182	1.07

τ (min) is the value of the specified time constant, determining z_p; $z_p = e^{-\frac{\tau}{T}}$
t_{err} (min) is the time when the hot-spot temperature error amounts to 63.2% of the initial value

$RMSE_{1\,h}$ is the root mean square of the bottom oil temperature error (*RMSE*), defined as $RMSE = \sqrt{\frac{1}{N}\sum_{i=1}^{N} \Delta\theta_{boi}^2}$, during the first hour
$\Delta\theta_{bo\,max}$ is the maximum difference of bottom oil temperature calculated by the observer and in the "System" structure

Table 2. The influence of non-ideal modelling and measuring noise

τ (min)	$t_{er\,r}$ (min)	$RMSE_{1\,h}$ (K)	$RMSE_{24\,h}$ (K)	$RMSE_{1\,h\,max}$ (K)	h_{max}	$\Delta\theta_{bo\,max}$ (K)	$\Delta\theta_{hs\,max > 1h}$ (K)
5	10.67	0.497	0.490	0.868	7	3.33	25.1
10	16.33	0.592	0.553	1.03	6	3.93	14.0
15	17.33	0.806	0.694	1.45	6	3.94	11.6
20	17.67	1.08	0.911	2.00	6	4.45	11.1
No observer	21.33	1.90	2.21	4.40	3	7.22	7.28

$RMSE_{24\,h}$ is *RMSE* during the whole 24-h period
$RMSE_{1\,h\,max}$ is the maximum *RMSE* value during 1 h
h_{max} is the hour in which $RMSE_{1\,h\,max}$ is reached
$\Delta\theta_{hs\,max > 1\,h}$ is the maximum difference of observed and measured hot-spot temperatures, excluding the first hour

Table 3. Test results: the change of parameters in the transformer model

x	$RMSE_{24\ h}$ (K)	$RMSE_{1h\ ma}$ (K)	h_{max}	$RMSE_{1\ h}$ (K)	$\Delta\theta_{bo\ max}$ (K)	$\Delta\theta_{hs\ max > 1\ h}$ (K)
$\Lambda_1 = x16.224(\vartheta_{hs} - \vartheta_{bo})^{0.60454}$, $\Lambda_2 = 294.302$						
1	0.03507	0.00341	2	0.1718	0.292	0.104
0.9	0.0323	0.0189	6	0.1554	0.266	4.86
0.8	0.0311	0.0410	6	0.1369	0.237	10.7
0.7	0.0326	0.0673	6	0.1162	0.206	17.7
0.6	0.0381	0.0992	6	0.0933	0.172	26.5
$\Lambda_1 = 16.224(\vartheta_{hs} - \vartheta_{bo})^{0.60454}$, $\Lambda_2 = x294.302$						
0.9	0.08234	0.1201	7	0.2035	0.330	0.796
0.8	0.1650	0.2592	7	0.2381	0.369	1.73
0.7	0.2712	0.4220	8	0.2751	0.440	2.83
0.6	0.4078	0.6221	8	0.3141	0.644	4.14

x is the factor of thermal conductances modelling the worsening of the cooling system

Table 4. Test results: the change of parameters on the real transformer

x	$RMSE_{24\,h}$ (K)	$RMSE_{1h\,max}$ (K)	h_{max}	$RMSE_{1\,h}$ (K)	$\Delta\theta_{bo\,max}$ (K)	$\Delta\theta_{hs\,max\,>\,1\,h}$ (K)
$\Lambda_{1o}=x16.224(\vartheta_{hs}-\vartheta_{bo})^{0.60454}$, $\Lambda_{2o}=294.302$						
1	0.5533	1.030	6	0.5923	3.93	14.0
1.11	0.5505	1.019	6	0.5846	3.91	9.3
1.25	0.5477	1.007	6	0.5763	3.89	10.1
1.43	0.5448	0.9946	6	0.5676	3.87	12.5
1.67	0.5419	0.9819	6	0.5584	3.84	15.6
$\Lambda_{1}=16.224(\vartheta_{hs}-\vartheta_{bo})^{0.60454}$, $\Lambda_{2}=x294.302$						
1.11	0.5551	1.084	6	0.6156	3.79	14.4
1.25	0.5707	1.162	6	0.6481	3.62	14.9
1.43	0.6097	1.274	6	0.6933	3.39	15.6
1.67	0.6875	1.440	6	0.7582	3.38	16.4

Table 5. Test results: the change of parameters without the observer

x	$RMSE_{24\,h}$ (K)	$RMSE_{1h\,ma}$ (K)	h_{max}	$RMSE_{1\,h}$ (K)	$\Delta\theta_{bo\,max}$ (K)	$\Delta\theta_{hs\,max}$ (K)
$\Lambda_{1o}=x16.224(\vartheta_{hs}-\vartheta_{bo})^{0.60454}$, $\Lambda_{2o}=294.302$						
1	2.210	4.401	3	1.901	7.22	7.28
1.11	2.166	4.279	3	1.837	7.09	7.16
1.25	2.119	4.152	3	1.765	6.95	11.3
1.43	2.070	4.020	3	1.686	6.80	15.5
1.67	2.019	3.883	3	1.599	6.64	19.9
$\Lambda_1=16.224(\vartheta_{hs}-\vartheta_{bo})^{0.60454}$, $\Lambda_2=x294.302$						
1.11	2.546	5.654	6	2.086	8.97	5.79
1.25	3.662	7.474	6	2.315	10.88	7.26
1.43	5.094	9.441	6	2.599	12.91	9.52
1.67	6.662	11.743	7	2.959	15.06	12.26